Discrete Spectrum of Interior Length and Timeshift in Two-sided Black Hole

Masamichi Miyaji

Yukawa Institute for Theoretical Physics, Kyoto University, Kyoto, 606-8267, Japan

E-mail: masamichi.miyaji@gmail.com

ABSTRACT: We study the spectrum of the interior length and the horizon timeshift of a two-sided black hole by constructing non-perturbative length and timeshift operators in Jackiew-Teitelboim gravity. We first construct projection operators onto the fixed length or fixed horizon timeshift subspaces using the replica trick. We calculate the densities of state for the length and the timeshift, which are found to be finite. This finiteness implies the discreteness in the spectrum of these quantities. We then construct the non-perturbative length and timeshift operators, and apply them to study the time evolution of the two-sided black hole. We find that at early time, the probability distribution of the interior length and the timeshift are sharply peaked at the classical values, while after the Heisenberg time, the distribution is completely uniform over all possible values of the length and the timeshift, indicating maximal uncertainty. In particular, the probability of having the negative timeshift states, which corresponds to the white hole probability, is $O(1)$ after the Heisenberg time.
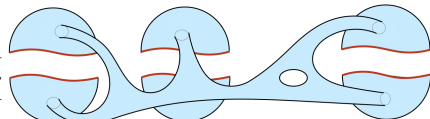
Contents

1 Introduction

Inclusion of Euclidean wormhole [1, 2] into the gravitational path-integral turned out to be powerful approach to study generic properties of quantum gravity, maintaining both intuitive spacetime geometry as well as the finiteness of the quantum gravity Hilbert space dimension [3–14]. Combining with the connection to the quantum entanglement [15–20], it is possible to extract bulk degrees of freedom from subregion of the AdS boundary [21–25] or the interior information from the Hawking radiation.

On the other hand, the existence of Euclidean wormholes implies that the gravity quantum states on fixed time slice geometry are not necessarily orthogonal with each other due to non-factorized geometry, even if they can never be connected via the change of slicing [10, 26, 27]. This is due to the effect of baby universe emission, which can change the geometry of the timeslice [1, 2, 10], or equivalently due to the presence of null states [1, 28, 29]. The gravitational path-integral with Euclidean wormholes in AdS is dual to ensemble averaging over boundary theories [3, 30, 31], and corresponds to the ensemble average over microscopic gravity theories in the bulk [32–34]. The ensemble average can indeed reproduce

typical behavior of the gravity theories in the ensemble such as the entropy of Hawking radiation [35] and the recoverability of the interior [36] by confirming the deviations are exponentially suppressed. It is possible to reproduce low energy density of states of near extremal black holes [37–40] as well as the factorization of bulk Hilbert space [41, 42].

The natural way to construct quantum gravity states with fixed timeslice geometry is to use an extension of the Hartle-Hawking prescription [43]. We denote the values of geometric quantities as f, and corresponding geometric states as $|\Psi(f)\rangle$. Then the ensemble average of the product of overlaps between geometric states is

$$\mathbb{E}\Big[\langle \text{TFD}|\Psi(f_1)\rangle\langle\Psi(f_1')|\text{TFD}\rangle\cdots\Big] = \sum_{\text{Wormholes}} {}^{f_1}_{f_1'} \; \cdots \; {}^{f_n}_{f_n'} .$$

(1.1)

Here the sum is over all possible Euclidean wormhole contributions with fixed boundary geometry. In particular, the Euclidean wormholes do not change the topology of the timeslice. The effect of Euclidean wormholes is that $\langle\Psi(f)|\Psi(f')\rangle$ is no longer orthogonal even if it was so in the absence of Euclidean wormholes. The immediate consequence is that the notion of the geometry of timeslice becomes ambiguous as an observable since it is no longer an eigenvalue of a Hermitian operator due to the non-orthogonality mentioned above. The same issue appeared in the end-of-the-world brane models of black holes, which have many excitations behind horizon that are highly non-orthogonal with each other [8, 44, 45].

The non-orthogonality of these geometric states is necessary and is universal, since the number of geometric states is continuously infinite while the entropy of a black hole is finite, requiring a huge over-completeness in the geometric states. If $|\Psi(f)\rangle$ with f contained in a finite interval $[f_1, \ f_2]$ can span the entire Hilbert space, it is impossible to have a Hermitian operator $\hat{F}$ which satisfies $\hat{F}|\Psi(f)\rangle \approx f|\Psi(f)\rangle$ for all values of f. This is because $|\Psi(f)\rangle$ with $f \notin [f_1, \ f_2]$ cannot satisfy this approximate equality. Thus, in this case, we can at most impose $\hat{F}|\Psi(f)\rangle \approx f|\Psi(f)\rangle$ for $f \in [f_1, \ f_2]$ or for even smaller range of f.

In this paper, we construct such Hermitian operators for the length of geodesic timeslice and the timeshift in a two-sided black hole in two-dimensional Jackiew-Teitelboim gravity [4, 46–55], and show that the spectrum of the both geometric quantities are *discrete*.

The length of the geodesic time slice is identical to the volume of the Einstein-Rosen (ER) bridge, which has been of great interest in terms of the exploration of the black hole interior [26, 27, 56, 57] as well as relation to the gravity dual of the quantum state complexity [58–62] and the Fisher information metric [63–65]. The volume of the ER bridge in a two-sided black hole has been expected to grow linearly in time until it reaches the maximal value of order e^{S_0} from the quantum complexity perspective, which has been confirmed in [26] for JT gravity. In this paper, we will construct the length operator explicitly and compute the probability distribution of the length, *which is completely free from divergence* that was present in the previous studies. We find that for early time, the length probability distribution is sharply peaked at the semiclassical value, thus the semiclassical approximation is valid. While *at late time, the probability distribution is constant over all possible values of length, implying maximal uncertainty in the length.*

We also considered the timeshift at the black hole horizon. This is the canonical conjugate of the two-sided Hamiltonian [54], which has played an important role in the recent studies on the algebraic structure of the black hole horizon [66–72]. As was proposed in [57], the timeshift can be used to measure the "age" of the two-sided black hole, capturing the tunneling from the black hole into the white hole via emission of baby universes [56]. In this paper, we construct a non-perturbative timeshift operator. Similar to the length operator, the probability distribution peaked at the semiclassical value at the early time while becoming uniform at the late time. In particular, the probability of finding the white hole and black hole at the late time are equal, showing that the old two-sided black hole is a superposition of black holes and white holes, confirming the idea of "grey hole" proposed in [73].

The organization of this paper is as follows. In section 2, we consider length and timeshift states ignoring the non-orthogonality. In section 3, we explain how discrete spectrum appears and how to construct the non-perturbative length/timeshift operator. In section 4, we apply these non-perturbative operators to understand the late-time interior quantum geometry of the two-sided black hole. We will see that the probability distribution for length becomes flat. We also see that the black and white hole probabilities are equal.

Note Added

After this paper was finalized, we noticed interesting upcoming work [74], which is based on a distinct construction but contains similar results. It would be very interesting to understand how their construction is related to ours.

2   Non-orthogonal Geometric States

In this section, we will construct non-orthogonal geometric states based on the extended Hartle-Hawking prescription. It turns out the geodesic length state and the timeshift state are special and can be written without referring to the microscopic Hamiltonian.

The bulk single-sided Hamiltonian of JT gravity in the disk topology is

$$H = \frac{P^2}{2} + 2e^{-L}, \tag{2.1}$$

where L is the regularized length of the geodesic timeslice, and P is the conjugate momentum of L [48, 54]. Since we have $P = i[H, L] = \dot{L}$, the physical meaning of P is the expansion speed of the length of the geodesic timeslice. Here we set the boundary value of the dilaton as $\phi_b = 1$ to simplify notation. Note that the pure JT gravity the energy of the left and right boundaries are equal and Hilbert spaces do not factorize [54]. Thus whenever we denote the energy E in this paper, we will mean by the two-sided energy which is the double of the single-sided one. The density of states at the disk level is

$$\rho_{\text{Disk}}(E) = e^{S_0} D_{\text{Disk}}(E) = e^{S_0} \frac{\sinh(2\pi\sqrt{E})}{4\pi^2}. \tag{2.2}$$

The wavefuncitons of L eigenstates can be obtained by solving $-\partial_l^2 \psi + 4e^{-l}\psi = E\psi$, and one finds

$$\psi_{\text{Disk},L}(E,l) = e^{-S_0/2}2^{3/2}K_{i2\sqrt{E}}(2e^{-l/2}). \tag{2.3}$$

Similarly, the wavefunctions of $P = \dot{L}$ eigenstates are

$$\psi_{\text{Disk},P}(E,p) = e^{-S_0/2}2\Gamma[i(\sqrt{E}-p)]\Gamma[-i(\sqrt{E}+p)]. \tag{2.4}$$

In this paper, we will consider the microcanonical ensemble, with a sharp energy window

$$E \in \left[E_0 - \frac{\Delta E'}{2}, \ E_0 + \frac{\Delta E'}{2}\right]. \tag{2.5}$$

Assuming $\Delta E'$ is small, the total Hilbert space dimension N' is finite and can be approximated as

$$N' \approx e^{S_0}D_{\text{Disk}}(E_0)\Delta E'. \tag{2.6}$$

2.1 Geodesic Length States

Let us denote the microscopic spectrum of the two-sided Hamiltonian as E_i. We consider the overlap between the unnormalized thermofield double state $|\text{TFD}(\beta)\rangle = \sum_i e^{-\beta E_i/4}|E_i\rangle$ and the geometric state $|\Psi(f)\rangle$. For some special family of timeslices and associated geometric quantities, the gravitational path-integral for the product of $\langle\Psi(f)|\text{TFD}(\beta)\rangle$s and their conjugates is related to that of the product of $\langle\text{TFD}(\beta')|\text{TFD}(\beta)\rangle = Z((\beta+\beta')/2)$, independently from microscopic Hamiltonians. For example, in the case of the fixed geodesic length timeslice in JT gravity [27, 69], each gravitational configuration with geodesic timeslice can be related to the path-integral with circular AdS boundaries via

$$\mathbb{E}\left[\left(\int_{-\infty}^{\infty} dl \ \psi_{\text{Disk},L}(\beta,l)\langle\Psi(l)|\text{TFD}(\beta')\rangle\right)\cdots\right] = \mathbb{E}\left[\langle\text{TFD}(\beta)|\text{TFD}(\beta')\rangle\cdots\right]. \tag{2.7}$$

Here $\psi_{\text{Disk},L}(\beta,l) = \int dE e^{S_0}D_{\text{Disk}}(E)e^{-\beta E/4}\psi_{\text{Disk},L}(E,l)$ is the gravitational path-integral in disk topology, with boundary condition composed of fixed geodesic length l and fixed renormalized AdS boundary length $\beta/2$. This constraint is fulfilled when

$$|\text{TFD}(\beta)\rangle = \int dl \ \psi_{\text{Disk},L}(\beta,l)|l\rangle, \tag{2.8}$$

which can be solved by setting[1]

$$|l\rangle = \sum_{|E_i-E_0|<\Delta E'/2} \psi_{\text{Disk},L}(E_i,l)|E_i\rangle. \tag{2.10}$$

---

[1]It is convenient to use

$$\int_{-\infty}^{\infty} dl \ K_{i\sqrt{2E}}(2e^{-l/2})K_{i\sqrt{2E'}}(2e^{-l/2}) = \frac{\delta(E-E')}{8D_{\text{Disk}}(E)}, \tag{2.9}$$
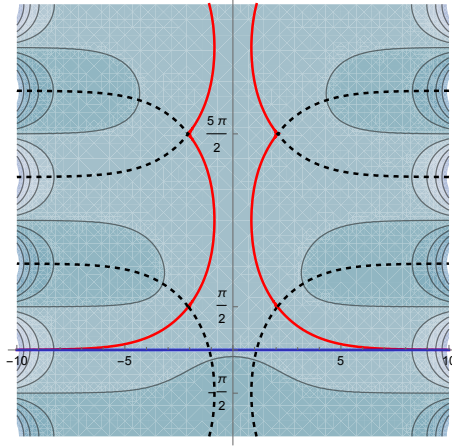
.

Figure 1: Change of integration contour in $\psi_{\mathrm{Disk}}(E, l)$ in the complex b plane. Along the dotted black curves and solid red curves, the imaginary part of the integrand is constant. The saddle points for the real part are located at intersections of these lines. We can deform the contour on the real line (solid blue) to the solid red curve. The real part of the integrand (darker blue describes the greater real part) on the red line is maximal at the saddles with $\mathrm{Im}\, b = \pi/2$, thus they dominate the whole integral at large $\sqrt{E} e^{l/2}$.

The states for the conjugate momentum P are given by

$$|p\rangle = \sum_{|E_i - E_0| < \Delta E'/2} \psi_{\mathrm{Disk},P}(E_i, p) |E_i\rangle. \tag{2.11}$$

It is natural to interpret $|l\rangle$ as the eigenvectors of the length operator. However, once we include the effect of baby universe corrections, these states are no longer orthogonal to each other. This implies that the operator L which satisfies $L|l\rangle = l|l\rangle$, cannot be a Hermitian operator and thus is not an observable, i.e. does not give well-defined probability distribution. This issue will be addressed in the next section.

From now on we study properties of the fixed geodesic length wave function $\psi_{\mathrm{Disk},L}(E, l)$ for large Ee^l. First, we rewrite the wavefunction as

$$\psi_{\mathrm{Disk},L}(E, l) = e^{-S_0/2} 2^{3/2} \int_{-\infty}^{\infty} db \, \exp\left(2ib\sqrt{E} - 2e^{-l/2}\cosh b\right). \tag{2.12}$$

The saddle points for this integral are

$$b_0 = \pm\mathrm{arccosh}(\sqrt{E}e^{l/2}) + \frac{\pi i}{2}(1 + 2m), \quad (m \in \mathbb{Z}). \tag{2.13}$$

The integrand around the saddle is, with $b = b_0 + \delta b$ and $m = 0$,

$$\exp\left(-\pi\sqrt{E} \mp 2ie^{-l/2}\sqrt{e^l E - 1} \pm 2i\sqrt{E}\mathrm{arccosh}(e^{l/2}\sqrt{E}) + ie^{-l/2}\sqrt{e^l E - 1}(\delta b)^2\right). \tag{2.14}$$

The integration contour can be deformed into a constant phase contour, and the real part

of the integrand is maximal at saddle points with $m = 0$. Incorporating the Gaussian integral around the saddles, we finally obtain, at large $\sqrt{E}e^{l/2}$,

$$\psi_{\text{Disk},L}(E,l) \to \frac{1}{\sqrt{\pi e^{S_0}D(E_0)}E_0^{1/4}} \cos\left(\sqrt{E}(l + \log 4E - 2) - \frac{\pi}{4}\right). \tag{2.15}$$

Here we defined

$$t_l := \frac{l + \log(4E_0)}{2\sqrt{E_0}}. \tag{2.16}$$

Note that the phase comes from the Jacobian $\text{Arg}[\delta b] = \pm\pi/4$. Let us further assume $(t_l - E_0^{-1/2})(\Delta E')^2 \ll E_0$, then we can expand inside the exponential and obtain

$$\psi_{\text{Disk},L}(E,l) \to \frac{1}{\sqrt{\pi e^{S_0}D(E_0)}E_0^{1/4}} \cos\left(\left[\sqrt{E_0}(l + \log(4E_0) - 2) - 2\sqrt{E_0} - \frac{\pi}{4}\right] + t_l(E - E_0)\right). \tag{2.17}$$

Later, we will take $t_l = O(e^{S_0}D(E_0))$. Thus the condition is equivalent to

$$\Delta E' \ll \sqrt{\frac{E_0}{e^{S_0}D(E_0)}}, \tag{2.18}$$

therefore the microcanonical window must be sufficiently small. Using the above expression, we obtain the overlap between fixed-length states

$$\begin{aligned}
\langle l|l'\rangle &= \sum_{|E_i - E_0| < \Delta E'/2} \psi_{\text{Disk},L}(E_i, l)\psi_{\text{Disk},L}(E_i, l') \\
&\approx \int_{E_0 - \Delta E'/2}^{E_0 + \Delta E'/2} dE\ e^{S_0}D(E_1)\psi_{\text{Disk},L}(E_i, l)\psi_{\text{Disk},L}(E_i, l') \\
&\approx \frac{1}{\pi E_0^{1/2}}\left(\frac{\cos\left(\sqrt{E_0}(l - l')\right)\sin\left((t_l - t_{l'})\Delta E'/2\right)}{t_l - t_{l'}}\right. \\
&\quad + \left.\frac{\sin\left(\sqrt{E_0}(l + l' + 2\log(4E_0) - 4) - \frac{\pi}{2}\right)\sin\left((t_l + t_{l'})\Delta E'/2\right)}{t_l + t_{l'}}\right).
\end{aligned} \tag{2.19}$$

In particular, the normalization of these states is

$$\langle l|l\rangle \underset{t_l \gg 1}{\to} \frac{\Delta E'}{2\pi\sqrt{E_0}}, \tag{2.20}$$

which is independent of l.

In the following, we will consider the microcanonical TFD state

$$|\text{TFD}(t)\rangle = N^{-1/2} \sum_{|E_i - E_0| < \Delta E/2} e^{-iE_i t}|E_i\rangle, \tag{2.21}$$

where

$$N \approx e^{S_0}D_{\text{Disk}}(E_0)\Delta E \approx e^{S_0}\frac{e^{2\pi\sqrt{E}}}{8\pi^2}\Delta E. \tag{2.22}$$

Here we used another microcanonical window which is a subset of the original one, so $\Delta E < \Delta E'$. This state is identical to the fixed δ state except for the distinct width for the energy window. We quote the result for the overlap of the fixed length states at the disk level with the TFD state. It is given by [75]

$$\frac{\langle \mathrm{TFD}(t)|l\rangle\langle l|\mathrm{TFD}(t)\rangle}{\langle l|l\rangle} \rightarrow \frac{2}{\Delta E \Delta E'}\left[\frac{\sin^2\left((t_l-t)\frac{\Delta E}{2}\right)}{\left(t_l-t\right)^2} + \frac{\sin^2\left((t_l+t)\frac{\Delta E}{2}\right)}{\left(t_l+t\right)^2}\right]$$
$$+ \frac{\pi}{T_H^2 \Delta E'}\left[\mathrm{Min}\Big[T_H,\ |t_l-t|\Big] + \mathrm{Min}\Big[T_H,\ |t_l+t|\Big]\right]. \tag{2.23}$$

The Heisenberg time T_H is defined by

$$T_H = \frac{2\pi}{\Delta E'}N' = 2\pi e^{S_0} D_{\mathrm{Disk}}(E_0). \tag{2.24}$$

It is natural to interpret $\langle \mathrm{TFD}(t)|l\rangle\langle l|\mathrm{TFD}(t)\rangle/\langle l|l\rangle$ as the probability distribution for the length. However $|l\rangle$ are not orthogonal to each other already at the disk level for small $|t_l - t_{l'}|$, and for any $|t_l - t_{l'}|$ once we include baby universe corrections. Thus the distribution does not define a probability distribution. Indeed, (2.23) cannot be normalized and is constant for any $|t_l| \gg t$. Our strategy in the next section is to define the new fixed geodesic length states and the length operator by projecting out shorter length states from the given length state at the disk level.

2.2 Timeshift States

The bulk one-sided Hamiltonian H is the conjugate momentum of the timeshift $\delta = \frac{t_R + t_L}{2}$. The wavefunction of δ eigenstates is

$$\psi_{\mathrm{Disk},\delta}(E,\delta) = \frac{e^{-i\delta E}}{\sqrt{e^{S_0}D_{\mathrm{Disk}}(E)}}, \tag{2.25}$$

and the fixed δ state in the microcanonical ensemble is

$$|\delta\rangle = \sum_{|E_i - E_0| < \Delta E'/2} \psi_{\mathrm{Disk},\delta}(E_i,\delta)|E_i\rangle, \tag{2.26}$$

which is nothing but the time-evolved microcanonical TFD state which is determined by the data of the energy eigenstates. Thus the product of overlaps can be related to the multi-boundary gravitational path-integral straightforwardly. The overlaps are

$$\langle \delta|\delta'\rangle = \sum_{|E_i - E_0| < \Delta E'/2} \psi_{\mathrm{Disk},\delta}(E_i,\delta)^* \psi_{\mathrm{Disk},\delta}(E_i,\delta')$$
$$= \int_{E_0-\Delta E'/2}^{E_0+\Delta E'/2} dE\, e^{S_0} D(E_1)\psi_{\mathrm{Disk},\delta}(E_1,\delta)^* \psi_{\mathrm{Disk},\delta}(E_1,\delta') \tag{2.27}$$
$$= \int_{E_0-\Delta E'/2}^{E_0+\Delta E'/2} dE_1\, e^{i(\delta-\delta')E_1} = 2e^{i(\delta-\delta')E_0}\frac{\sin\left((\delta-\delta')\Delta E'/2\right)}{\delta - \delta'}.$$

In particular, the normalization of this state is

$$\langle \delta | \delta \rangle = \Delta E'. \qquad (2.28)$$

The normalization is independent from δ.

We note that at the limit of $E_0 e^l \gg 1$ and $\Delta E' \ll \sqrt{\frac{E_0}{e^{S_0} D(E_0)}}$, decomposing the fixed length state into positive and negative P state gives fixed δ states with $\delta = t_l$ and $\delta = -t_l$. Because $\dot{L} = -i\partial_L$ is the canonical conjugate of L in JT gravity, the exact decomposition of the wavefunction into positive and negative P is

$$\begin{aligned}
\psi_{\text{Disk}}^{P>0}(E, l) &:= \frac{1}{2\pi} \int_0^\infty ds \ e^{-ils} \int_{-\infty}^\infty dl' \ e^{il's} \psi_{\text{Disk}}(E, l'), \\
\psi_{\text{Disk}}^{P<0}(E, l) &:= \frac{1}{2\pi} \int_{-\infty}^0 ds \ e^{-ils} \int_{-\infty}^\infty dl' \ e^{il's} \psi_{\text{Disk}}(E, l').
\end{aligned} \qquad (2.29)$$

They are indeed proportional to fixed δ wavefunctions at large Ee^l, with $\delta = t_l$ for $P > 0$ and $\delta = -t_l$ for $P < 0$

$$\begin{aligned}
\psi_{\text{Disk}}^{P>0}(E, l) &\approx \frac{1}{\sqrt{4\pi e^{S_0} D(E_0)} E_0^{1/4}} e^{-i\left[\sqrt{E_0}(l+\log(4E_0)-2)-\frac{\pi}{4}\right] - it_l(E-E_0)} \propto \psi_{\text{Disk},\delta}(E, t_l), \\
\psi_{\text{Disk}}^{P<0}(E, l) &\approx \frac{1}{\sqrt{4\pi e^{S_0} D(E_0)} E_0^{1/4}} e^{i\left[\sqrt{E_0}(l+\log(4E_0)-2)-\frac{\pi}{4}\right] + it_l(E-E_0)} \propto \psi_{\text{Disk},\delta}(E, -t_l).
\end{aligned} \qquad (2.30)$$

Finally, let us review the overlap of these states with the time-evolved thermofield double state. It is given by [75]

$$\frac{\langle \text{TFD}(t)|\delta\rangle\langle\delta|\text{TFD}(t)\rangle}{\langle\delta|\delta\rangle} \to \frac{4}{\Delta E \Delta E'} \frac{\sin^2\left((\delta - t)\frac{\Delta E}{2}\right)}{(\delta - t)^2} + \frac{2\pi}{T_H^2 \Delta E'} \text{Min}\left[T_H, \ |\delta - t|\right]. \qquad (2.31)$$

Again, we cannot interpret this distribution as a probability distribution for δ, since $|\delta\rangle$ are not orthogonal to each other already at the disk level in the microcanonical ensemble for small $|\delta - \delta'|$, and for arbitrary $|\delta - \delta'|$ due to baby universe corrections. Thus we see that the "time operator" $\hat{\delta}$ conjugate to the Hamiltonian cannot be a Hermitian operator in a finite system. This prohibits us from defining the timeshift operator naively using the fixed timeshift states. Our strategy is to define the new timeshift state by projecting out smaller timeshift states from the given fixed timeshift state at the disk level.

3 Discrete Spectrum of the Length and the Timeshift

In the previous section, we have constructed fixed length states and fixed timeshift states in the disk topology. These states are not orthogonal to each other due to the finiteness of the energy window and the baby universe corrections. In order to construct the orthogonal

length and timeshift basis, we consider the following positive semi-definite operators for $t_s > 0$ and $t_+, \ t_- > 0$ [2]

$$S^L[t_0, t_s] := \left(\frac{\Delta E'}{2\pi}\right) \int_{t_0}^{t_s} dt_l \ |l\rangle\langle l|,$$

$$S^\delta[-t_-, t_+] := \left(\frac{\Delta E'}{2\pi}\right) \int_{-t_-}^{t_+} d\delta \ |\delta\rangle\langle\delta|. \tag{3.1}$$

We further consider the subspace $H^L[t_0, t_s]$ and $H^\delta[-t_-, t_+]$ spanned by eigenvectors of $S^L[t_0, t_s]$ and $S^\delta[-t_-, t_+]$ with nonzero eigenvalues of order $O((e^{S_0})^0)$. The projection operators $P^L[t_0, t_s]$ and $P^\delta[-t_-, t_+]$ onto these subspaces can be obtained via

$$P^L[t_0, t_s] = S^L[t_0, t_s]^{+0},$$

$$P^\delta[-t_-, t_+] = S^\delta[-t_-, t_+]^{+0}, \tag{3.2}$$

with an understanding that we omit order e^{-S_0} eigenvalues before the the limit $n \to +0$ in the right hand side. Löwner–Heinz inequality tell us that there exist states $|l\rangle^\epsilon \approx |l\rangle$ and $|\delta\rangle^\epsilon \approx |\delta\rangle$ with small but possible $O((e^{-S_0})^0)$ error such that [3]

$$|l\rangle^\epsilon \in H^L[t_0, t_s] \ \ \text{for} \ \ t_l \in [t_0, t_s]$$

$$|\delta\rangle^\epsilon \in H^\delta[-t_-, t_+] \ \ \text{for} \ \ \delta \in [-t_-, t_+]. \tag{3.4}$$

We also have

$$H^L[t_0, t_s] \subset H^L[t_0, t_s'] \ \ \text{for} \ \ t_s \leq t_s'$$

$$H^\delta[-t_-, t_+] \subset H^\delta[-t_-', t_+'] \ \ \text{for} \ \ t_- \leq t_-', \ t_+ \leq t_+'. \tag{3.5}$$

Thus $H^L[t_0, t_s]$ and $H^\delta[-t_-, t_+]$ spanned by $|l\rangle^\epsilon$ with $t_0 < t_l < t_s$ and $|\delta\rangle^\epsilon$ with $-t_- < \delta < t_+$ respectively. Since these operators are projectors onto finite dimensional Hilbert space, by introducing *baby universe corrected* length and timeshift states $|\tilde{l}_i\rangle$ and $|\tilde{\delta}_i\rangle$, the projector can be written as

$$P^L[t_0, t_s] = \sum_{i: \ t_0 < t_{l_i} < t_s} |\tilde{l}_i\rangle\langle\tilde{l}_i|,$$

$$P^\delta[-t_s, t_s] = \sum_{i: \ -t_s < \delta_i < t_s} |\tilde{\delta}_i\rangle\langle\tilde{\delta}_i|. \tag{3.6}$$

---

[2]More generally, we can consider one parameter family $f_{t_s}(l)$ and $f_{t_s}(\delta)$ of non-negative real functions satisfying $f_{t_s}(l) \leq f_{t_s'}(l)$ and $f_{t_s}(\delta) \leq f_{t_s'}(\delta)$ to consider

$$S_f^L[t_0, t_s] := \left(\frac{\Delta E'}{2\pi}\right) \int_{-\infty}^{\infty} dt_l \ f_{t_s}(l)|l\rangle\langle l|,$$

$$S_f^\delta[-t_-, t_+] = \left(\frac{\Delta E'}{2\pi}\right) \int_{-\infty}^{\infty} d\delta \ f_{t_s}(\delta)|\delta\rangle\langle\delta|.$$

The subspaces $H_f^L[t_0, t_s]$ and $H_f^\delta[-t_s, t_s]$ are spanned by $|l\rangle$ with $f_{t_s}(l) \neq 0$ and $|\delta\rangle$ with $f_{t_s}(\delta) \neq 0$ respectively. Thus, the precise form of f_{t_s} should not matter in the rest of the paper.

[3]We consider $e^{-S_0} \ll \epsilon \ll 1$

$$\left(\frac{\Delta E'}{2\pi}\right) \int_{t_s}^{t_s + \epsilon} dt_l \ |l\rangle\langle l|, \ \left(\frac{\Delta E'}{2\pi}\right) \int_{t_s}^{t_s + \epsilon} d\delta \ |\delta\rangle\langle\delta|, \ \left(\frac{\Delta E'}{2\pi}\right) \int_{-t_s - \epsilon}^{-t_s} d\delta \ |\delta\rangle\langle\delta|, \tag{3.3}$$

and defined their eigenstate as $|l\rangle^\epsilon$, $|t_s\rangle^\epsilon$, $|-t_s\rangle^\epsilon$.

The new spectrum l_i and δ_i are interpreted as the baby universe corrected spectrum of the length and the timeshift. Importantly, these spectrums are *discrete*. States $|\tilde{l}_i\rangle$ and $|\tilde{\delta}_i\rangle$ are distinct from the length and timeshift states at the disk level, and form *orthonormal basis* of the Hilbert space [4].

We can think of the above process as a Gram-Schmidt orthogonalization procedure, applied in the following way

$$(|l_0\rangle^\epsilon,\ |l_1\rangle^\epsilon,\cdots) \to (|\tilde{l}_0\rangle = |l_0\rangle^\epsilon,\ |\tilde{l}_1\rangle,\cdots),\ (l_i < l_{i+1}),$$
$$(|\delta_0\rangle^\epsilon,\ |\delta_1\rangle^\epsilon,\cdots) \to (|\tilde{\delta}_0\rangle = |\delta_0\rangle^\epsilon,\ |\tilde{\delta}_1\rangle,\cdots),\ (|\delta_i| < |\delta_{i+1}|). \tag{3.7}$$

Here the Gram-Schmidt orthonormalization is performed starting from the reference state $|l_0\rangle$ with $t_{l_1} = t_0$ to a longer length state. In other words, shorter length states are projected out to obtain $|\tilde{l}_i\rangle$. For the fixed timeshift state, the orthonormalization is performed from the reference state at $\delta = 0$ to larger $|\delta|$.

3.1 Rank of the Projectors and Density of States

We evaluate the Renyi version of the rank of operators $S^L[t_0, t_s]$ and $S^\delta[-t_-, t_+]$ via

$$\mathrm{Tr}\Big[S^L[t_0, t_s]^n\Big],\ \mathrm{Tr}\Big[S^\delta[-t_-, t_+]^n\Big]. \tag{3.8}$$

To evaluate them, we consider

$$
\begin{aligned}
Y^L(E_a, E_b : [t_0, t_s]) &:= \langle E_a|S^L[t_0, t_s]|E_b\rangle = \int_{t_0}^{t_s}\left(\frac{\Delta E'}{2\pi}\right)dt_l\ \langle E_a|l\rangle\langle l|E_b\rangle \\
&= \int_{t_0}^{t_s}\left(\frac{\Delta E'}{2\pi}\right)dt_l\ \frac{2^2\pi e^{-2\pi\sqrt{E_0}-S_0}}{E_0^{1/2}}\Big(\cos\left(t_l(E_a - E_b)\right) \\
&\quad + \cos\left(2\left[\sqrt{E_0}(l + \log(4E_0) - 2) - \frac{\pi}{4}\right] + 2t_l(\frac{E_a + E_b}{2} - E_0)\right)\Big) \\
&\approx \left(\frac{\Delta E'}{4\pi^2 e^{S_0}D(E_0)E_0^{1/2}}\right)\frac{\sin\left((E_a - E_b)t_s\right) - \sin\left((E_a - E_b)t_0\right)}{E_a - E_b},
\end{aligned} \tag{3.9}
$$

here we ignored the second term in the integral. We also consider

$$
\begin{aligned}
Y^\delta(E_a, E_b : [-t_-, t_+]) &:= \langle E_a|S^\delta[-t_-, t_+]|E_b\rangle = \int_{-t_-}^{t_+}\left(\frac{\Delta E'}{2\pi}\right)d\delta\ \langle E_a|\delta\rangle\langle\delta|E_b\rangle \\
&= \left(\frac{\Delta E'}{\pi e^{S_0}D(E_0)}\right)\frac{e^{i(E_a - E_b)t_-} - e^{-i(E_a - E_b)t_+}}{2i(E_a - E_b)}.
\end{aligned} \tag{3.10}
$$

Using these quantities, we can express

$$
\begin{aligned}
\mathrm{Tr}\Big[S^L[t_0, t_s]^n\Big] &= \sum_{a_1,\cdots,a_{n+1}}\langle E_{a_1}|S^L(t_s)|E_{a_2}\rangle\langle E_{a_2}|S^L(t_s)|E_{a_3}\rangle\cdots\langle E_{a_n}|S^L(t_s)|E_{a_1}\rangle \\
&= \int_{E_0 - \Delta E'/2}^{E_0 + \Delta E'/2}dE_1\cdots dE_n\ Y^L(E_1, E_2)Y^L(E_2, E_3)\cdots Y^L(E_n, E_1) \\
&\quad \times e^{nS_0}\langle D(E_1)\cdots D(E_n)\rangle,
\end{aligned} \tag{3.11}
$$

---

[4]We note that in general $P^\delta[-t_-, t_+] \neq \sum_{i:\ -t_- < \delta_i < t_+}|\tilde{\delta}_i\rangle\langle\tilde{\delta}_i|$.

For S^δ, replace Y^L by Y^δ. We can evaluate these by approximating the density of states correlation function by using the random matrix universality. Namely, when the energy difference is small, we can approximate the density of state correlation function by the sine kernel

$$K(E_i, E_j) = \frac{\sin\left(\pi e^{S_0} D(E_0)(E_i - E_j)\right)}{\pi(E_i - E_j)}, \tag{3.12}$$

via the relation from random matrix theory

$$
\begin{aligned}
&e^{nS_0}\langle D(E_1)\cdots D(E_n)\rangle \\
&= \sum_{(1,\cdots,N)=(a_1^{(1)}, a_2^{(1)}\cdots)+\cdots} \left(\Pi_i \delta(E_{a_1^{(1)}}, E_{a_2^{(1)}}\cdots)\right) R_p(E_{a_1^{(1)}}, E_{a_1^{(2)}}\cdots),
\end{aligned}
\tag{3.13}
$$

here the sum is over all possible partition of $(1, \cdots, N)$, counting equivalent partition only once. We defined

$$\delta(E_1, \cdots, E_m) := \delta(E_1 - E_2)\delta(E_2 - E_3)\cdots\delta(E_{m-1} - E_m), \tag{3.14}$$

and

$$R_k(E_1, \cdots, E_k) = \det_{i,j=1,\cdots,k} K(E_i, E_j). \tag{3.15}$$

We also note that we often approximate an integral over rescaled energy difference $u = (E_1 - E_2)e^{S_0}$ by an integral over the whole real line, so that the contour integrals can be done conveniently. We thus implicitly assume that $\Delta E' \gg e^{-S_0}$. See also [26, 75].

Short Interval Limit

Let us consider the case when t_0, t_s, t_-, $t_+ \ll T_H$. Then the dominant contribution comes from the disconnected contribution, namely the approximation $\langle D(E_1)\cdots D(E_{n+1})\rangle \approx \langle D(E_1)\rangle\cdots\langle D(E_{n+1})\rangle$ is valid. This contribution is nothing but the semiclassical one. Then we obtain [5]

$$
\begin{aligned}
\mathrm{Tr}\left[S^L[t_0, t_s]^{+0}\right] &= \frac{t_s - t_0}{\pi}\Delta E', \\
\mathrm{Tr}\left[S^\delta[-t_-, t_+]^{+0}\right] &= \frac{t_- + t_+}{2\pi}\Delta E'.
\end{aligned}
\tag{3.18}
$$

This result is remarkable and implies that *the density of geometric states is finite and constant in the microcanonical ensemble.*

---

[5]It is convenient to use, for A, $|B| \geq 0$ with $x_1 \neq x_3$ that

$$\int_{-\infty}^{\infty} dx_2 \frac{e^{iA(x_1-x_2)} - e^{-iB(x_1-x_2)}}{2i(x_1-x_2)} \frac{e^{iA(x_2-x_3)} - e^{-iB(x_2-x_3)}}{2i(x_2-x_3)} = \pi \frac{e^{iA(x_1-x_3)} - e^{-iB(x_1-x_3)}}{2i(x_1-x_3)}, \tag{3.16}$$

and for $A, B > 0$

$$\int_{-\infty}^{\infty} dx_2 \frac{\sin(A(x_1-x_2))}{x_1-x_2} \frac{\sin(B(x_2-x_3))}{x_2-x_3} = \pi \frac{\sin(\mathrm{Min}[A, B](x_1-x_3))}{x_1-x_3}. \tag{3.17}$$

And when $x_1 = x_3$, the first expression becomes $\frac{\pi}{2}(A + B)$, and the second expression becomes $\mathrm{Min}[A, B]$.

First Correction from Finite Width

We incorporate large t_0, t_s, t_-, t_+ correction perturbatively. The correction is given by

$$\mathrm{Tr}\Big[S^L[t_0, t_s]^n\Big]^{(1)} = e^{2S_0}\Big(\frac{\Delta E'}{4E_0^{1/2}}\Big)^{n-2}\frac{n(n-1)}{2}$$
$$\times \int_{E_0-\Delta E'/2}^{E_0+\Delta E'/2} dE_1 dE_2 \ Y^L(E_1, E_2)Y^L(E_2, E_1)\langle D(E_1)D(E_2)\rangle_{\mathrm{c}}. \tag{3.19}$$

For O^δ, replace Y^L by Y^δ. Here we defined

$$\langle D(E_1)D(E_2)\rangle_{\mathrm{c}} := \langle D(E_1)D(E_2)\rangle - \langle D(E_1)\rangle\langle D(E_2)\rangle$$
$$\approx e^{-S_0}\delta(E_2 - E_3)D_{\mathrm{Disk}}(E_1) - e^{-2S_0}\frac{\sin^2(\pi e^{S_0}D_{\mathrm{Disk}}(E_0)(E_2 - E_3))}{\pi^2(E_2 - E_3)^2}. \tag{3.20}$$

We conclude that the first correction vanishes

$$\mathrm{Tr}\Big[S^L[t_0, t_s]^{+0}\Big]^{(1)} = \mathrm{Tr}\Big[S^\delta[-t_-, t_+]^{+0}\Big]^{(1)} = 0. \tag{3.21}$$

Long Interval Limit

Let us next consider the case when $t_s - t_0$, t_-, $t_+ \gg T_H$. Then the dominant contribution comes from the fully connected delta function contribution, namely the approximation $\langle D(E_1)\cdots D(E_{n+1})\rangle \approx e^{-nS_0}D(E_1)\delta(E_1 - E_2)\delta(E_2 - E_3)\cdots\delta(E_n - E_{n+1})$ is valid. Then we can conclude that the rank is maximal

$$\mathrm{Tr}\Big[S^L[t_0, t_s]^{+0}\Big] = \mathrm{Tr}\Big[S^\delta[-t_-, t_+]^{+0}\Big] = e^{S_0}D(E_0)\Delta E' = N'. \tag{3.22}$$

Density of States

In this paper, we have only computed dominant contributions to the density of geometric states in extreme cases. The absence of the first correction from the finite width effect, suggests that the result at the short interval limit can be interpolated for a finite interval until the total number of states saturates the long interval limit. Assuming this behavior, we estimate that the full density of state

$$\rho(t_s : t_0) \approx \frac{\Delta E'}{\pi}\theta(\frac{T_H}{2} - t_s), \ (t_s > t_0),$$
$$\rho([-t_-, t_+]) \approx \frac{\Delta E'}{2\pi}\theta(\frac{T_H}{2} - t_+)\theta(\frac{T_H}{2} - t_-), \ (t_-, t_+ > 0). \tag{3.23}$$

In other words, *the density of geometric states is finite and constant in the microcanonical ensemble until the total number of states equals the Hilbert space dimension.* The Heaviside theta function in the expression is included in order to be consistent with the long interval limit and to match the Hilbert space dimension. Note that the density of states above depends on what we choose the reference state, such as t_0 in $\rho(t_s : t_0)$ and $\delta = 0$ in $\rho([-t_-, t_+])$.

3.2 Non-perturbative Length and Timeshift Operators

Using the spectrum and the baby universe corrected geometric states, we can construct non-perturbative geometric operators. The non-perturbative geodesic length operator and timeshift operator can be constructed via

$$\hat{L}^{\text{NP}} := \sum_i l_i |\tilde{l}_i\rangle\langle\tilde{l}_i|, \quad \hat{\delta}^{\text{NP}} := \sum_i \delta_i |\tilde{\delta}_i\rangle\langle\tilde{\delta}_i|. \tag{3.24}$$

These operators indeed approximate the disk level length and timeshift operators for $|l\rangle$ with $t_l \approx t_0$ and $|\delta\rangle$ with small δ, since in that regime we still have $|\tilde{l}\rangle \approx |l\rangle$ and $|\tilde{\delta}\rangle \approx |\delta\rangle$. While for large l' or $|\delta|$, the deviation from the disk level geometric state can be large and such approximation is no longer valid.

4 Dynamics of the Einstein-Rosen Bridge

In the following, we use the above non-perturbative length and timeshift operators to analyze the late time behavior of the thermofield double state. For this purpose, it suffices to evaluate the Renyi version of the projection amplitude

$$\begin{aligned}
Q^L(n, t_0, t_s) &= \langle\text{TFD}(t)|S^L(t_0, t_s)^n|\text{TFD}(t)\rangle, \\
Q^\delta(n, t_-, t_+) &= \langle\text{TFD}(t)|S^\delta(t_-, t_+)^n|\text{TFD}(t)\rangle,
\end{aligned} \tag{4.1}$$

at $n \to +0$. This projection amplitude is written as

$$\begin{aligned}
Q^L(n, t_0, t_s) &= \sum_{a_1, \cdots, a_{n+1}} \langle\text{TFD}(t)|E_{a_1}\rangle\langle E_{a_1}|S^L(t_s)|E_{a_2}\rangle \cdots \langle E_{a_n}|S^L(t_s)|E_{a_{n+1}}\rangle\langle E_{a_{n+1}}|\text{TFD}(t)\rangle \\
&= \mathcal{N}^{-1} \int_{E_0-\Delta E/2}^{E_0+\Delta E/2} dE_1 dE_{n+1} \int_{E_0-\Delta E'/2}^{E_0+\Delta E'/2} dE_2 \cdots dE_n \, e^{i(E_1-E_{n+1})t} \\
&\quad \times Y^L(E_1, E_2) \cdots Y^L(E_n, E_{n+1}) e^{(n+1)S_0} \langle D(E_1) \cdots D(E_{n+1})\rangle.
\end{aligned} \tag{4.2}$$

For Q^δ, replace Y^L by Y^δ. The length probability density can then be obtained by taking t_s derivative

$$P^L(t_l) = \frac{d}{dt_s}\Big|_{t_s=t_l} Q^L(+0, t_0, t_s). \tag{4.3}$$

The timeshift probability density is expressed as

$$\begin{aligned}
P_+^\delta(\delta) &= \frac{d}{dt_+}\Big|_{t_+=t_-=\delta} Q^\delta(+0, t_-, t_+) \; (\delta > 0), \\
P_-^\delta(\delta) &= \frac{d}{dt_-}\Big|_{t_+=t_-=-\delta} Q^\delta(+0, t_-, t_+) \; (\delta < 0).
\end{aligned} \tag{4.4}$$

Note $t_- = t_+$ is imposed in this expression. We note that when $t_s := t_- = t_+$ and $t_0 = 0$, we have $Y^L \propto Y^\delta$. Thus the equality between the length and $|\delta|$ probability holds

$$Q^\delta(+0, t_s, t_s)^{(0+1)} = Q^L(+0, 0, t_s)^{(0+1)}. \tag{4.5}$$

The probability of finding a black hole and a white hole are,

$$P^{\mathrm{BH}}(t) = \int_0^{T_H/2} d\delta' \ P^+(\delta'),$$

$$P^{\mathrm{WH}}(t) = \int_{-T_H/2}^0 d\delta' \ P^-(\delta').$$

(4.6)

Large t_l and $|\delta|$

Let us first consider the case when $t_s - t_0$, t_-, $t_+ \gg T_H$. Then the dominant contribution comes from the fully connected delta function contribution, namely the approximation $\langle D(E_1) \cdots D(E_{n+1}) \rangle \approx e^{-nS_0} D(E_1) \delta(E_1 - E_2) \delta(E_2 - E_3) \cdots \delta(E_n - E_{n+1})$ is valid for Y^L, and $\langle D(E_1) \cdots D(E_n) \rangle \approx e^{-(n-1)S_0} D(E_1) \delta(E_1 - E_2) \delta(E_2 - E_3) \cdots \delta(E_{n-1} - E_n)$ is for Y^δ. Then we have

$$Q^L(0, t_0, t_s) = Q^\delta(0, t_-, t_+) = 1,$$

(4.7)

consistent with the probabilistic reasoning.

4.1 Length of the Einstein-Rosen Bridge

Small t_s

Let us consider the case when $t_0, t_s \ll T_H$. Then the dominant contribution comes from the disconnected contribution. This is nothing but the semiclassical contribution. Thus we obtain

$$Q^L(0, t_0, t_s)^{(0)} = \theta(t + t_s) - \theta(t + t_0) - \theta(t - t_s) + \theta(t - t_0).$$

(4.8)

We thus have

$$P^L(0, t_0, t_s)^{(0)} = \delta(t + t_s) + \delta(t - t_s),$$

(4.9)

which matches the classical length of the Einstein-Rosen bridge.

First Correction from Finite $(t_s - t_0)/T_H$

Next, we study the first correction from $(t_s - t_0)/T_H$ expansion. For this purpose, we include the two-body correlation to the density of state correlation function. We find for $t > 0$ and $T_H/2 > t_s > t_0 > 0$ that

$$Q^L(+0, t_0, t_s)^{(1)} = -\Big(\theta(t - t_0) - \theta(t - t_s)\Big) \frac{t^2 - 2t_0 t + t_s^2}{T_H^2}$$
$$+ \int_{t_0}^{t_s} dt_l \frac{1}{T_H^2} \Big(\mathrm{Min}\Big[T_H, \ |t_l - t|\Big] + \mathrm{Min}\Big[T_H, \ |t_l + t|\Big]\Big).$$

(4.10)

The detailed derivation is given in appendix A.1. Let us examine the detailed behavior of $Q^L(+0, t_0, t_s)^{(0)+(1)}$. For simplicity, we approximate as $t_0 \approx 0$ in the following. Then we
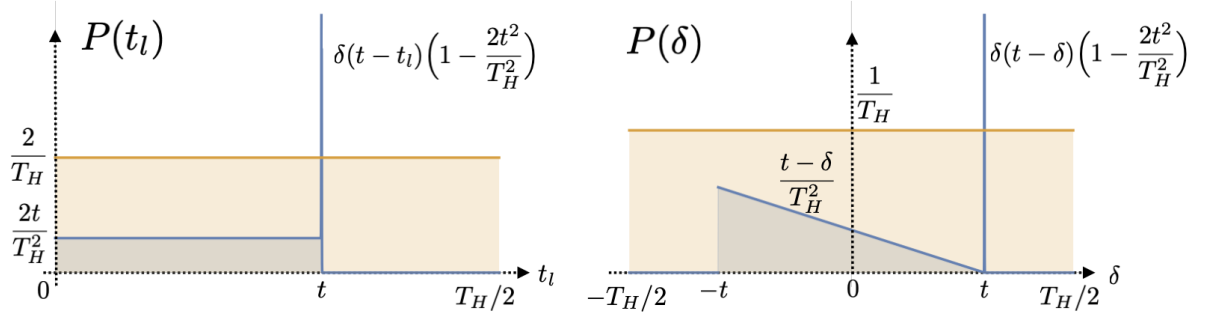
Figure 2: The density of states of the length l and the timeshift δ. The blue curve is for $t < T_H/2$, and the orange curve is for $t > 3T_H/2$. (Left) The density of states of the length states. When $t < T_H/2$, the density has a delta function peak at the classical value. From the wormhole effect, the length is distributed over *shorter value uniformly*. When $t > 3T_H/2$, the probability is completely uniform. (Right) The density of states of the timeshift states. When $t < T_H/2$, the density has a delta function peak at the classical value, and the timeshift is linearly distributed for $|\delta| < t$. Again when $t > 3T_H/2$, the probability distribution is uniform.

can simplify

$$Q^L(+0, 0, t_s)^{(0+1)} = 1 + \theta(t - t_s)\left(-1 + \frac{2tt_s}{T_H^2}\right)$$
$$+ \frac{1}{2T_H^2}\left(\theta(t - t_s - T_H)(t - t_s - T_H)^2 - \theta(t + t_s - T_H)(t + t_s - T_H)^2\right).$$
(4.11)

The length probability distribution is

$$P(t_l)^{(0+1)} = \delta(t - t_l)\left(1 - \frac{2t^2}{T_H^2}\right) + \theta(t - t_l)\frac{2t}{T_H^2}$$
$$- \frac{1}{T_H^2}\left(\theta(t - t_l - T_H)(t - t_l - T_H) + \theta(t + t_l - T_H)(t + t_l - T_H)\right).$$
(4.12)

Result: Early time $t < T_H/2$:

The probability distribution is given by

$$P(t_l)^{(0+1)} = \delta(t - t_l)\left(1 - \frac{2t^2}{T_H^2}\right) + \theta(t - t_l)\frac{2t}{T_H^2}.$$
(4.13)

Thus we have

$$Q^L(+0, 0, t_s)^{(0+1)} = 1 - \theta(t - t_s) + \theta(t - t_s)\frac{2tt_s}{T_H^2}.$$
(4.14)

– 15 –

Which is 1 for $t_s > t$, which is consistent with the probabilistic interpretation for $t_s = T_H/2$. Thus in this order, we can see that the baby universe only shortens the classical geodesic time slice, and does not give rise to a longer Einstein-Rosen bridge. The probability of having a shorter ER bridge with $t_l > 0$ is uniform. The expectation value of length and its variance are

$$\mathbb{E}[t_l]^{(0+1)} = t - \frac{t^3}{T_H^2}, \quad \sqrt{\mathbb{E}\left[(t_l - \mathbb{E}[t_l])^2\right]}^{(0+1)} = \frac{t^2}{T_H}\sqrt{\frac{2}{3} - \frac{t^2}{T_H^2}}. \tag{4.15}$$

Thus, at the early time, the length expectation value is slightly shorter than the classical value, and the variance is suppressed as $T_H^{-1/2}$. Therefore the usual approximation by classical gravity is still valid.

Result: Late time $T_H/2 < t$:

The probability distribution is given by

$$P(t_l)^{(0+1)} = \frac{2t}{T_H^2} - \frac{1}{T_H^2}\Big(\theta(t - t_l - T_H)(t - t_l - T_H) + \theta(t + t_l - T_H)(t + t_l - T_H)\Big). \tag{4.16}$$

Let us focus on the case $3T_H/2 < t$. Then we have

$$P(t_l)^{(0+1)} = \frac{2}{T_H}, \quad Q^L(+0, 0, t_s)^{(0+1)} = \frac{2t_s}{T_H}. \tag{4.17}$$

$Q^L(+0, 0, t_s)^{(0+1)}$ becomes 1 when $t_s = T_H/2$, and the density of length is uniform. The expectation value of length and its variance are

$$\mathbb{E}[t_l]^{(0+1)} = \frac{T_H}{4}, \quad \sqrt{\mathbb{E}\left[(t_l - \mathbb{E}[t_l])^2\right]}^{(0+1)} = \frac{T_H}{4\sqrt{3}}. \tag{4.18}$$

Thus the length expectation value is independent from time t and is significantly shorter than the classical value. The variance is of the same order as the length expectation value. To account for the intermediate time $T_H/2 < t < 3T_H/2$, the current leading order calculation is not sufficient and we need higher order calculations.

4.2 Timeshift at the Black Hole Horizon

Small t_-, t_+

Let us consider the case when t_-, $t_+ \ll T_H$. Then the dominant contribution comes from the disconnected contribution. Thus

$$Q^\delta(0, t_-, t_+)^{(0)} = \theta(t + t_-) - \theta(t - t_+). \tag{4.19}$$

We thus have

$$P_+^\delta(0, \delta)^{(0)} = \delta(t - \delta), \quad P_-^\delta(0, \delta)^{(0)} = \delta(t + \delta). \tag{4.20}$$

Again we reproduce the classical expectation.

First Correction from Finite $(t_s - t_0)/T_H$

The first correction from $(t_s - t_0)/T_H$ expansion for $Q(+0, t, t_-, t+)$ is, for $0 < t, t_-, t_+$ and $t_- + t_+ < T_H$,

$$Q^\delta(+0, t_-, t_+)^{(1)} = -\theta(-t + t_+)\Big(t^2 + t(t_- - t_+) + \frac{t_-^2 + t_+^2}{2}\Big)\frac{1}{T_H^2}$$
$$+ \int_{-t_-}^{t_+} d\delta \, \frac{1}{T_H^2}\text{Min}\Big[T_H, \, |\delta - t|\Big]. \tag{4.21}$$

see appendix A.2 for more detailed calculations. Let us examine the detailed behavior of $Q^\delta(+0, t_-, t_+)^{(0)+(1)}$. The probability distribution for δ is

$$P^+(\delta)^{(0+1)} = \delta(t - \delta)\Big(1 - \frac{2t^2}{T_H^2}\Big) - \theta(\delta - t)\frac{\delta - t}{T_H^2} + \frac{1}{T_H^2}\text{Min}\Big[T_H, \, |\delta - t|\Big],$$
$$P^-(\delta)^{(0+1)} = -\theta(-t - \delta)\frac{t - \delta}{T_H^2} + \frac{1}{T_H^2}\text{Min}\Big[T_H, \, |\delta - t|\Big]. \tag{4.22}$$

Result: Early time $t < T_H/2$**:**

The probability distribution is

$$P^+(\delta)^{(0+1)} = \delta(t - \delta)\Big(1 - \frac{2t^2}{T_H^2}\Big) + \frac{1}{T_H^2}\theta(t - \delta)(t - \delta),$$
$$P^-(\delta)^{(0+1)} = \theta(t + \delta)\frac{t - \delta}{T_H^2}. \tag{4.23}$$

The integrated probability, which corresponds to the BH and WH respectively, is

$$P^{\text{BH}}(t) = 1 - \frac{3t^2}{2T_H^2}, \quad P^{\text{WH}}(t) = \frac{3t^2}{2T_H^2}. \tag{4.24}$$

The expectation value of the timeshift and its variance are

$$\mathbb{E}[\delta]^{(0+1)} = t\Big(1 - \frac{8t^2}{3T_H^2}\Big), \quad \sqrt{\mathbb{E}\Big[(\delta - \mathbb{E}[\delta])^2\Big]^{(0+1)}} = \frac{2t^2}{T_H}\sqrt{1 + \frac{16t^2}{3T_H^2}}. \tag{4.25}$$

Result: Late time $t > T_H/2$**:**

The probability distribution is

$$P^+(\delta)^{(0+1)} = \frac{1}{T_H^2}\text{Min}\Big[T_H, \, |\delta - t|\Big],$$
$$P^-(\delta)^{(0+1)} = \frac{1}{T_H^2}\text{Min}\Big[T_H, \, |\delta - t|\Big]. \tag{4.26}$$

When $t > 3T_H/2$, then we have

$$P^+(\delta)^{(0+1)} = P^-(\delta)^{(0+1)} = \frac{1}{T_H}, \tag{4.27}$$

and thus

$$P^{\text{BH}}(t) = P^{\text{WH}}(t) = \frac{1}{2}, \tag{4.28}$$

indicating equal probability between a black hole and a white hole at the late time. The expectation value of the timeshift and its variance are

$$\mathbb{E}[\delta]^{(0+1)} = 0, \ \sqrt{\mathbb{E}\left[(\delta - \mathbb{E}[\delta])^2\right]^{(0+1)}} = \frac{T_H}{2\sqrt{3}}. \tag{4.29}$$

Again, to account for the intermediate time $T_H/2 < t < 3T_H/2$, we need higher order calculations.

5 Discussions

In this paper, we constructed non-perturbative length and timeshift operators. It turned out that their spectrum is discrete in accord with the dimensionality of the microcanonical Hilbert space. By considering the timeshift operator, we confirmed that the late-time TFD state is the mixture of the black hole and white hole states with equal probability. The most urgent future direction is to fully incorporate the finite $(t_s - t_0)/T_H$ and t_s/T_H effects into the density of states and the probability distribution, in order to justify our results at late time. We expect the construction described in this paper can be applied to general bulk geometric quantities, such as the Wheeler-de-Witt action [76]. Furthermore, we can analyze the *discrete* version of the algebraic structure at the horizon as well as the density of geometric states in various backgrounds including de Sitter space. It would also be interesting to understand the relation to approaches to Hartle-Hawking wavefunction from Liouville action [61, 62, 77, 78] and $T\bar{T}$ deformation [79]. We conclude with further comments and future directions.

Relation to Other Definitions of Length

In [56], the minimal length geodesic timeslice was considered to define the probability distribution as well as transition probability into a white hole. Although the current approach is similar to theirs, the final results are somewhat different; we can compare the results for probability distribution (4.13), (4.23), and the white hole probability (4.24). Our results indicate that transition into shorter wormholes has constant probability in t_l as can be seen in (4.13), (4.23) and in (4.24), while in [56], the probability is proportional to $(t - t_l)$. It is very interesting to understand the origin of this difference and give a detailed geometric understanding of our approach. Note that there is no contradiction here, as the two approaches are not equivalent.

The nice feature of the current construction of a non-perturbative geometric operator is that it is free from divergence. The divergence can come from the constant overlap with arbitrary long length and timeshift state as displayed in (2.23) and (2.31), which leads to

divergence of the total probability and thus expectation value of geometric quantities[6]. In our case the spectrum of the length and the timeshift are finite, and the total probability is normalized, therefore such divergence does not arise.

Dependence on the Reference State

The non-perturbative length operator depends on the reference state in order to construct the basis of geometric states from that reference state. The most remarkable feature is that geometric interpretation can drastically depend on the choice of the basis. If we consider the short ER bridge basis, then at a sufficiently late time, the overlap with the TFD state spread homogeneously over the basis and there is no classical fixed length timeslice at all as we saw in the body of this paper. On the other hand, if we consider the long ER bridge basis, then there was no classical fixed length timeslice at early times, yet at some point in the late time, classical geometry suddenly emerged out of nowhere. Similarly, in the short ER bridge basis, the probability of having a white hole is small at an early time and becomes $1/2$ at a late time. On the other hand, on the long ER bridge basis, the probability of finding a white hole is $1/2$ at an early time and becomes small at some point in the late time. It would be very interesting to understand the bulk physical implications of such reference dependence.

Probes for Generic Quantum Systems

The construction of our non-perturbative length and the timeshift operator has a close resemblance to the spread complexity [80–83]. In the spread complexity, one acts Hamiltonian to the initial state multiple times to create a set of states and applies the Gram-Schmidt orthogonalization to these states to construct a basis for the (sub)space. In the current case, we instead fix the reference state and construct projectors onto $O(1)$ eigenvalues of positive semi-definite operators $S^L[t_0, t_s]$ and $S^\delta[-t_-, t_+]$. More generally, we can consider the subspace spanned by $O(1)$ eigenvalue eigenstates of the time-averaged density matrix

$$\bar{\rho}[0, T] := \frac{1}{T} \int_0^T dt \ \rho(t), \tag{5.1}$$

and construct the orthonormal basis $|\tilde{T}_i\rangle$ of the Hilbert space. Using that basis, we can construct the "time" operator

$$\hat{T} := \sum_i \tilde{T}_i |\tilde{T}_i\rangle\langle\tilde{T}_i|. \tag{5.2}$$

It would be very interesting to explore various relations further and compute these quantities in generic quantum systems.

---

[6]Note that neither the length state nor the timeshift state give the resolution of identity. As we can see by integrating over l or δ of (2.23) and (2.31), we can see

$$\int_{-\infty}^\infty dl \ |l\rangle\langle l| \neq \mathbb{I}, \quad \int_{-\infty}^\infty d\delta \ |\delta\rangle\langle\delta| \neq 2\pi\mathbb{I},$$

because the left-hand sides of the two equations are *divergent* for any time-evolved TFD state. The equalities (5.1) hold at the disk level, but fail badly once we include the baby universe corrections. Note that, unlike many other cases, the disk answer is not even close to the ensemble-averaged answer.

Acknowledgments

A Detailed Calculation of the Corrections

A.1 Length

We present detailed calculations of finite $(t_s - t_0)/T_H$ correction to the Q^L and O^L. The correction is

$$
Q^L(n, t_k)^{(1)} = \mathcal{N}^{-1} e^{4S_0} \left(\frac{\Delta E'}{4\pi E_0^{1/2}} \right)^{n-3} \int_{E_0 - \Delta E/2}^{E_0 + \Delta E/2} dE_1 dE_{n+1} \int_{E_0 - \Delta E'/2}^{E_0 + \Delta E'/2} dE_2 dE_3 \; e^{i(E_1 - E_{n+1})t}
$$

$$
\times \frac{(n-1)(n-2)}{2} Y(E_1, E_2) Y(E_2, E_3) Y(E_3, E_{n+1}) D(E_1) \langle D(E_2) D(E_3) \rangle_{\rm c} D(E_{n+1})
$$

$$
+ \mathcal{N}^{-1} e^{3S_0} \left(\frac{\Delta E'}{4\pi E_0^{1/2}} \right)^{n-2} \int_{E_0 - \Delta E/2}^{E_0 + \Delta E/2} dE_1 dE_{n+1} \int_{E_0 - \Delta E'/2}^{E_0 + \Delta E'/2} dE_2 \; e^{i(E_1 - E_{n+1})t}
$$

$$
\times (n-1) Y(E_1, E_2) Y(E_2, E_{n+1}) \Big(\langle D(E_1) D(E_2) \rangle_{\rm c} D(E_{n+1}) + D(E_1) \langle D(E_2) D(E_{n+1}) \rangle_{\rm c} \Big)
$$

$$
+ \mathcal{N}^{-1} e^{2S_0} \left(\frac{\Delta E'}{4\pi E_0^{1/2}} \right)^{n-1} \int_{E_0 - \Delta E/2}^{E_0 + \Delta E/2} dE_1 dE_{n+1} \; e^{i(E_1 - E_{n+1})t} Y(E_1, E_{n+1}) \langle D(E_1) D(E_{n+1}) \rangle_{\rm c}.
$$

$$(A.1)$$

We assume $t > 0$. The first term is

$$
\mathcal{N}^{-1} e^{S_0} \left(\frac{\Delta E'}{4\pi E_0^{1/2}} \right)^{n-1} \int_{E_0 - \Delta E/2}^{E_0 + \Delta E/2} dE_1 dE_{n+1} \; e^{i(E_1 - E_{n+1})t} \frac{(n-1)(n-2)}{2} Y(E_1, E_{n+1}) D(E_{n+1}) \frac{t_s - t_0}{\pi}
$$

$$
- \mathcal{N}^{-1} e^{2S_0} \left(\frac{\Delta E'}{4\pi E_0^{1/2}} \right)^{n-3} \int_{E_0 - \Delta E/2}^{E_0 + \Delta E/2} dE_1 dE_{n+1} \int_{E_0 - \Delta E'/2}^{E_0 + \Delta E'/2} dE_2 dE_3 \; e^{i(E_1 - E_{n+1})t}
$$

$$
\times \frac{(n-1)(n-2)}{2} Y(E_1, E_2) Y(E_2, E_3) Y(E_3, E_{n+1}) D(E_1) \frac{\sin^2 \left(\pi e^{S_0} D(E_2)(E_2 - E_3) \right)}{\pi^2 (E_2 - E_3)^2} D(E_{n+1})
$$

$$
= \frac{(n-1)(n-2)}{2} \left(\frac{\Delta E'}{4\pi E_0^{1/2}} \right)^{n} \Big(\theta(t - t_0) - \theta(t - t_s) \Big) \frac{t^2 - 2tt_0 + t_k^2}{T_H^2}.
$$

$$(A.2)$$

The second term is

$$\mathcal{N}^{-1}e^{S_0}\Big(\frac{\Delta E'}{4\pi E_0^{1/2}}\Big)^{n-1}\int_{E_0-\Delta E/2}^{E_0+\Delta E/2}dE_1 dE_{n+1}\ e^{i(E_1-E_{n+1})t}2(n-1)Y(E_1,E_{n+1})D(E_{n+1})\frac{t_s-t_0}{\pi}$$

$$-\mathcal{N}^{-1}e^{S_0}\Big(\frac{\Delta E'}{4\pi E_0^{1/2}}\Big)^{n-2}\int_{E_0-\Delta E/2}^{E_0+\Delta E/2}dE_1 dE_{n+1}\int_{E_0-\Delta E'/2}^{E_0+\Delta E'/2}dE_2\ e^{i(E_1-E_{n+1})t}$$

$$\times(n-1)Y(E_1,E_2)Y(E_2,E_{n+1})\frac{\sin^2\Big(\pi e^{S_0}D(E_2)(E_1-E_2)\Big)}{\pi^2(E_1-E_2)^2}D(E_{n+1})$$

$$-\mathcal{N}^{-1}e^{S_0}\Big(\frac{\Delta E'}{4\pi E_0^{1/2}}\Big)^{n-2}\int_{E_0-\Delta E/2}^{E_0+\Delta E/2}dE_1 dE_{n+1}\int_{E_0-\Delta E'/2}^{E_0+\Delta E'/2}dE_2\ e^{i(E_1-E_{n+1})t}$$

$$\times(n-1)Y(E_1,E_2)Y(E_2,E_{n+1})D(E_1)\frac{\sin^2\Big(\pi e^{S_0}D(E_2)(E_2-E_{n+1})\Big)}{\pi^2(E_2-E_{n+1})^2}$$

$$=2(n-1)\Big(\frac{\Delta E'}{4\pi E_0^{1/2}}\Big)^n\Big(\theta(t-t_0)-\theta(t-t_s)\Big)\frac{t^2-2tt_0+t_s^2}{T_H^2}. \tag{A.3}$$

The third term is

$$\Big(\frac{\Delta E'}{4\pi E_0^{1/2}}\Big)^n\Big[2\int_{t_0}^{t_s}dt_l\ \Big(\frac{\Delta E'}{2\pi}\Big)\frac{\langle\mathrm{TFD}(t)|t_l\rangle\langle t_l|\mathrm{TFD}(t)\rangle}{\langle t_l|t_l\rangle}-\Big(\theta(t_s-t)-\theta(t-t_0)\Big)\Big]$$

$$=\Big(\frac{\Delta E'}{4\pi E_0^{1/2}}\Big)^n\int_{t_0}^{t_s}dt_l\ \frac{1}{T_H^2}\Big[\mathrm{Min}\Big[T_H,\ |t_l-t|\Big]+\mathrm{Min}\Big[T_H,\ |t_l+t|\Big]\Big]. \tag{A.4}$$

More explicitly, it is equal to

$$\Big(\frac{\Delta E'}{4\pi E_0^{1/2}}\Big)^n\frac{1}{T_H^2}\Big(2T_H(t_s-t_0)+\theta(t-t_0)(t-t_0)^2-(t+t_0)^2$$

$$-\theta(t-t_0-T_H)(t-t_0-T_H)^2/2+\theta(t+t_0-T_H)(t+t_0-T_H)^2/2-\theta(t-t_0+T_H)(t-t_0+T_H)^2/2$$

$$+(t+t_0+T_H)^2/2-\theta(t-t_s)(t-t_s)^2+(t+t_s)^2+\theta(t-t_s-T_H)(t-t_s-T_H)^2/2$$

$$+\theta(t-t_s+T_H)(t-t_s+T_H)^2/2-\theta(t+t_s-T_H)(t+t_s-T_H)^2/2-(t+t_s+T_H)^2/2\Big). \tag{A.5}$$

Summing over these contribution, for $t>0$ and $T_H/2>t_s>t_0>0$, we have

$$Q^L(n,t_0,t_s)^{(1)}=\Big(\frac{\Delta E'}{4\pi E_0^{1/2}}\Big)^n\times\Big[\frac{(n-1)(n+2)}{2}\Big(\theta(t-t_0)-\theta(t-t_s)\Big)\frac{t^2-2t_0t+t_s^2}{T_H^2}$$

$$+\int_{t_0}^{t_s}dt_l\ \frac{1}{T_H^2}\Big(\mathrm{Min}\Big[T_H,\ |t_l-t|\Big]+\mathrm{Min}\Big[T_H,\ |t_l+t|\Big]\Big)\Big]. \tag{A.6}$$

For O^L, we have

$$O^L(n,t_k)^{(1)}=\Big(\frac{\Delta E'}{4\pi E_0^{1/2}}\Big)^n\frac{n(n-1)}{2}\Delta E'\frac{2}{3\pi}\frac{(t_s-t_0)^2(2t_s+t_0)}{T_H^2}. \tag{A.7}$$

A.2 Timeshift

We present detailed calculations of finite t_s/T_H correction to the Q^δ and O^δ. The correction is

$$
\begin{aligned}
Q^\delta(n,t,t_-,t+)^{(1)} = {} & \mathcal{N}^{-1} e^{4S_0} \left(\Delta E'\right)^{n-3} \int_{E_0-\Delta E/2}^{E_0+\Delta E/2} dE_1 dE_{n+1} \int_{E_0-\Delta E'/2}^{E_0+\Delta E'/2} dE_2 dE_3 \; e^{i(E_1-E_{n+1})t} \\
& \times \frac{(n-1)(n-2)}{2} Y(E_1,E_2)Y(E_2,E_3)Y(E_3,E_{n+1})D(E_1)\langle D(E_2)D(E_3)\rangle_{\mathrm{c}} D(E_{n+1}) \\
& + \mathcal{N}^{-1} e^{3S_0} \left(\Delta E'\right)^{n-2} \int_{E_0-\Delta E/2}^{E_0+\Delta E/2} dE_1 dE_{n+1} \int_{E_0-\Delta E'/2}^{E_0+\Delta E'/2} dE_2 \; e^{i(E_1-E_{n+1})t} \\
& \times (n-1) Y(E_1,E_2)Y(E_2,E_{n+1})\Big(\langle D(E_1)D(E_2)\rangle_{\mathrm{c}} D(E_{n+1}) + D(E_1)\langle D(E_2)D(E_{n+1})\rangle_{\mathrm{c}}\Big) \\
& + \mathcal{N}^{-1} e^{2S_0} \left(\Delta E'\right)^{n-1} \int_{E_0-\Delta E/2}^{E_0+\Delta E/2} dE_1 dE_{n+1} \; e^{i(E_1-E_{n+1})t} Y(E_1,E_{n+1})\langle D(E_1)D(E_{n+1})\rangle_{\mathrm{c}}.
\end{aligned}
$$

(A.8)

The first term is

$$
\begin{aligned}
& \mathcal{N}^{-1} e^{S_0} \left(\Delta E'\right)^{n-1} \int_{E_0-\Delta E/2}^{E_0+\Delta E/2} dE_1 dE_{n+1} \; e^{i(E_1-E_{n+1})t} \frac{(n-1)(n-2)}{2} Y(E_1,E_{n+1})D(E_{n+1})\frac{t_-+t_+}{2\pi} \\
& - \mathcal{N}^{-1} e^{2S_0} \left(\Delta E'\right)^{n-3} \int_{E_0-\Delta E/2}^{E_0+\Delta E/2} dE_1 dE_{n+1} \int_{E_0-\Delta E'/2}^{E_0+\Delta E'/2} dE_2 dE_3 \; e^{i(E_1-E_{n+1})t} \\
& \times \frac{(n-1)(n-2)}{2} Y(E_1,E_2)Y(E_2,E_3)Y(E_3,E_{n+1})D(E_1)\frac{\sin^2\left(\pi e^{S_0}D(E_2)(E_2-E_3)\right)}{\pi^2(E_2-E_3)^2}D(E_{n+1}) \\
& = \frac{(n-1)(n-2)}{2} \left(\Delta E'\right)^{n} \Big(\theta(t+t_-)-\theta(t-t_+)\Big)\left(t^2 + t(t_--t_+) + \frac{t_-^2+t_+^2}{2}\right)\frac{1}{T_H^2}.
\end{aligned}
$$

(A.9)

The second term is

$$
\begin{aligned}
& \mathcal{N}^{-1} e^{S_0} \left(\Delta E'\right)^{n-1} \int_{E_0-\Delta E/2}^{E_0+\Delta E/2} dE_1 dE_{n+1} \; e^{i(E_1-E_{n+1})t} 2(n-1) Y(E_1,E_{n+1})D(E_{n+1})\frac{t_-+t_+}{2\pi} \\
& - \mathcal{N}^{-1} e^{S_0} \left(\Delta E'\right)^{n-2} \int_{E_0-\Delta E/2}^{E_0+\Delta E/2} dE_1 dE_{n+1} \int_{E_0-\Delta E'/2}^{E_0+\Delta E'/2} dE_2 \; e^{i(E_1-E_{n+1})t} \\
& \times (n-1) Y(E_1,E_2)Y(E_2,E_{n+1})\frac{\sin^2\left(\pi e^{S_0}D(E_2)(E_1-E_2)\right)}{\pi^2(E_1-E_2)^2}D(E_{n+1}) \\
& - \mathcal{N}^{-1} e^{S_0} \left(\Delta E'\right)^{n-2} \int_{E_0-\Delta E/2}^{E_0+\Delta E/2} dE_1 dE_{n+1} \int_{E_0-\Delta E'/2}^{E_0+\Delta E'/2} dE_2 \; e^{i(E_1-E_{n+1})t} \\
& \times (n-1) Y(E_1,E_2)Y(E_2,E_{n+1})D(E_1)\frac{\sin^2\left(\pi e^{S_0}D(E_2)(E_2-E_{n+1})\right)}{\pi^2(E_2-E_{n+1})^2} \\
& = 2(n-1) \left(\Delta E'\right)^{n} \Big(\theta(t+t_-)-\theta(t-t_+)\Big)\left(t^2 + t(t_--t_+) + \frac{t_-^2+t_+^2}{2}\right)\frac{1}{T_H^2}.
\end{aligned}
$$

(A.10)

The third term is

$$
\left(\Delta E'\right)^n \Big[\int_{-t_-}^{t_+} dt_l \, \Big(\frac{\Delta E'}{2\pi}\Big) \frac{\langle \mathrm{TFD}(t)|\delta\rangle \langle \delta|\mathrm{TFD}(t)\rangle}{\langle \delta|\delta\rangle} - \Big(\theta(t+t_-) - \theta(t-t_+)\Big) \Big]
$$
$$
= \left(\Delta E'\right)^n \int_{-t_-}^{t_+} d\delta \, \frac{1}{T_H^2} \mathrm{Min}\Big[T_H, \; |\delta - t|\Big].
$$
(A.11)

More explicitly,

$$
\left(\Delta E'\right)^n \Big(\frac{t_- + t_+}{T_H} + \frac{1}{T_H^2}\Big(\theta(t+t_-)(t+t_-)^2 - \theta(t - T_H + t_-)(t - T_H + t_-)^2/2
$$
$$
- \theta(t + T_H + t_-)(t + T_H + t_-)^2/2 - \theta(t - t_+)(t - t_+)^2 + \theta(t - T_H - t_+)(t - T_H - t_+)^2/2
$$
$$
+ \theta(t + T_H - t_+)(t + T_H - t_+)^2/2\Big).
$$
(A.12)

A.3 Replica Calculations

We write the short and long-interval limit results for general n.

Short Interval Limit

When $t_0, \; t_s, \; t_-, \; t_+ \ll T_H$, we have

$$
Q^L(n, t_0, t_s)^{(0)} = \Big(\frac{\Delta E'}{4\pi E_0^{1/2}}\Big)^n \Big(\theta(t + t_s) - \theta(t + t_0) - \theta(t - t_s) + \theta(t - t_0)\Big),
$$
$$
O^L(n, t_0, t_s)^{(0)} = \Big(\frac{\Delta E'}{4\pi E_0^{1/2}}\Big)^n \frac{t_s - t_0}{\pi} \Delta E',
$$
$$
Q^\delta(n, t_-, t_+)^{(0)} = (\Delta E')^n \Big(\theta(t + t_-) - \theta(t - t_+)\Big),
$$
$$
O^\delta(n, t_-, t_+)^{(0)} = (\Delta E')^n \frac{t_- + t_+}{2\pi} \Delta E'.
$$
(A.13)

Long Interval Limit

When $t_s - t_0, \; t_-, \; t_+ \gg T_H$, we have

$$
Q^L(n, t_0, t_s) = \Big(\frac{(t_s - t_0)\Delta E'}{4\pi^2 e^{S_0} D(E_0) E_0^{1/2}}\Big)^n,
$$
$$
O^L(n, t_0, t_s) = \Big(\frac{(t_s - t_0)\Delta E'}{4\pi^2 e^{S_0} D(E_0) E_0^{1/2}}\Big)^n e^{S_0} D(E_0) \Delta E',
$$
$$
Q^\delta(n, t_-, t_+) = \Big(\frac{(t_- + t_+)\Delta E'}{2\pi e^{S_0} D(E_0)}\Big)^n,
$$
$$
O^\delta(n, t_-, t_+) = \Big(\frac{(t_- + t_+)\Delta E'}{2\pi e^{S_0} D(E_0)}\Big)^n e^{S_0} D(E_0) \Delta E'.
$$
(A.14)

A.4 Black and White hole probability

We write the black hole and white hole probability including the first correction from finite $(t_s - t_0)/T_H$ and t_s/T_H effect. They are given by

$$
\begin{aligned}
P^{\mathrm{BH}}(t)^{(0)+(1)} = \int_0^{T_H/2} d\delta' \; P^+(\delta')^{(0+1)} &= \theta(T_H/2 - t)\Big(1 - \frac{5t^2 - T_H t + T_H^2/4}{2T_H^2}\Big) \\
&+ \frac{1}{8} + \frac{1}{T_H^2}\Big(t^2 - tT_H/2 + \theta(t - T_H)(t - T_H)^2/2 \\
&- \theta(t - T_H/2)(t - T_H/2)^2 + \theta(t - 3T_H/2)(t - 3T_H/2)^2/2\Big), \\
P^{\mathrm{WH}}(t)^{(0)+(1)} = \int_{-T_H/2}^0 d\delta' \; P^-(\delta')^{(0+1)} &= \theta(T_H/2 - t)\frac{3t^2 - T_H t - T_H^2/4}{2T_H^2} \\
&+ \frac{1}{8} + \frac{1}{T_H^2}\Big(tT_H/2 - \theta(t - T_H/2)(t - T_H/2)^2/2 \\
&+ \theta(t - T_H)(t - T_H)^2/2\Big).
\end{aligned}
\tag{A.15}
$$

References

[1] S.R. Coleman, *Black holes as red herrings: Topological fluctuations and the loss of quantum coherence*, *Nucl. Phys. B* **307** (1988) 867.

[2] S.B. Giddings and A. Strominger, *Axion Induced Topology Change in Quantum Gravity and String Theory*, *Nucl. Phys. B* **306** (1988) 890.

[3] P. Saad, S.H. Shenker and D. Stanford, *A semiclassical ramp in SYK and in gravity*, 1806.06840.

[4] P. Saad, S.H. Shenker and D. Stanford, *JT gravity as a matrix integral*, 1903.11115.

[5] G. Penington, *Entanglement Wedge Reconstruction and the Information Paradox*, *JHEP* **09** (2020) 002 [1905.08255].

[6] A. Almheiri, N. Engelhardt, D. Marolf and H. Maxfield, *The entropy of bulk quantum fields and the entanglement wedge of an evaporating black hole*, *JHEP* **12** (2019) 063 [1905.08762].

[7] A. Almheiri, R. Mahajan, J. Maldacena and Y. Zhao, *The Page curve of Hawking radiation from semiclassical geometry*, *JHEP* **03** (2020) 149 [1908.10996].

[8] G. Penington, S.H. Shenker, D. Stanford and Z. Yang, *Replica wormholes and the black hole interior*, *JHEP* **03** (2022) 205 [1911.11977].

[9] A. Almheiri, T. Hartman, J. Maldacena, E. Shaghoulian and A. Tajdini, *Replica Wormholes and the Entropy of Hawking Radiation*, *JHEP* **05** (2020) 013 [1911.12333].

[10] P. Saad, *Late Time Correlation Functions, Baby Universes, and ETH in JT Gravity*, 1910.10311.

[11] K. Okuyama and K. Sakai, *Multi-boundary correlators in JT gravity*, *JHEP* **08** (2020) 126 [2004.07555].

[12] A. Blommaert, J. Kruthoff and S. Yao, *An integrable road to a perturbative plateau*, *JHEP* **04** (2023) 048 [2208.13795].

[13] P. Saad, D. Stanford, Z. Yang and S. Yao, *A convergent genus expansion for the plateau*, 2210.11565.

[14] K. Okuyama and K. Sakai, *Spectral form factor in the τ-scaling limit*, *JHEP* **04** (2023) 123 [2301.04773].

[15] S. Ryu and T. Takayanagi, *Holographic derivation of entanglement entropy from AdS/CFT*, *Phys. Rev. Lett.* **96** (2006) 181602 [hep-th/0603001].

[16] V.E. Hubeny, M. Rangamani and T. Takayanagi, *A Covariant holographic entanglement entropy proposal*, *JHEP* **07** (2007) 062 [0705.0016].

[17] T. Faulkner, A. Lewkowycz and J. Maldacena, *Quantum corrections to holographic entanglement entropy*, *JHEP* **11** (2013) 074 [1307.2892].

[18] T. Hartman and J. Maldacena, *Time Evolution of Entanglement Entropy from Black Hole Interiors*, *JHEP* **05** (2013) 014 [1303.1080].

[19] A. Lewkowycz and J. Maldacena, *Generalized gravitational entropy*, *JHEP* **08** (2013) 090 [1304.4926].

[20] D.L. Jafferis, A. Lewkowycz, J. Maldacena and S.J. Suh, *Relative entropy equals bulk relative entropy*, *JHEP* **06** (2016) 004 [1512.06431].

[21] B. Czech, J.L. Karczmarek, F. Nogueira and M. Van Raamsdonk, *The Gravity Dual of a Density Matrix*, *Class. Quant. Grav.* **29** (2012) 155009 [1204.1330].

[22] F. Pastawski, B. Yoshida, D. Harlow and J. Preskill, *Holographic quantum error-correcting codes: Toy models for the bulk/boundary correspondence*, *JHEP* **06** (2015) 149 [1503.06237].

[23] D. Harlow, *The Ryu–Takayanagi Formula from Quantum Error Correction*, *Commun. Math. Phys.* **354** (2017) 865 [1607.03901].

[24] X. Dong, D. Harlow and A.C. Wall, *Reconstruction of Bulk Operators within the Entanglement Wedge in Gauge-Gravity Duality*, *Phys. Rev. Lett.* **117** (2016) 021601 [1601.05416].

[25] C. Akers, N. Engelhardt, D. Harlow, G. Penington and S. Vardhan, *The black hole interior from non-isometric codes and complexity*, *JHEP* **06** (2024) 155 [2207.06536].

[26] L.V. Iliesiu, M. Mezei and G. Sárosi, *The volume of the black hole interior at late times*, *JHEP* **07** (2022) 073 [2107.06286].

[27] L.V. Iliesiu, A. Levine, H.W. Lin, H. Maxfield and M. Mezei, *On the non-perturbative bulk Hilbert space of JT gravity*, 2403.08696.

[28] D. Marolf and H. Maxfield, *Transcending the ensemble: baby universes, spacetime wormholes, and the order and disorder of black hole information*, *JHEP* **08** (2020) 044 [2002.08950].

[29] D. Marolf and H. Maxfield, *Observations of Hawking radiation: the Page curve and baby universes*, *JHEP* **04** (2021) 272 [2010.06602].

[30] R. Bousso and M. Tomašević, *Unitarity From a Smooth Horizon?*, *Phys. Rev. D* **102** (2020) 106019 [1911.06305].

[31] R. Bousso and E. Wildenhain, *Gravity/ensemble duality*, *Phys. Rev. D* **102** (2020) 066005 [2006.16289].

[32] P. Saad, S. Shenker and S. Yao, *Comments on wormholes and factorization*, 2107.13130.

[33] A. Blommaert, L.V. Iliesiu and J. Kruthoff, *Gravity factorized*, *JHEP* **09** (2022) 080 [2111.07863].

[34] A. Blommaert, L.V. Iliesiu and J. Kruthoff, *Alpha states demystified — towards microscopic models of AdS₂ holography*, *JHEP* **08** (2022) 071 [2203.07384].

[35] R. Bousso and M. Miyaji, *Fluctuations in the entropy of Hawking radiation*, *Phys. Rev. D* **109** (2024) 026006 [2307.13920].

[36] M. Miyaji and K. Yano, *Fluctuation in the fidelity of information recovery from Hawking radiation*, *Phys. Rev. D* **109** (2024) 086011 [2311.02881].

[37] L.V. Iliesiu and G.J. Turiaci, *The statistical mechanics of near-extremal black holes*, *JHEP* **05** (2021) 145 [2003.02860].

[38] M. Heydeman, L.V. Iliesiu, G.J. Turiaci and W. Zhao, *The statistical mechanics of near-BPS black holes*, *J. Phys. A* **55** (2022) 014004 [2011.01953].

[39] L.V. Iliesiu, S. Murthy and G.J. Turiaci, *Black hole microstate counting from the gravitational path integral*, 2209.13602.

[40] J. Boruch, L.V. Iliesiu and C. Yan, *Constructing all BPS black hole microstates from the gravitational path integral*, *JHEP* **09** (2024) 058 [2307.13051].

[41] J. Boruch, L.V. Iliesiu, G. Lin and C. Yan, *How the Hilbert space of two-sided black holes factorises*, 2406.04396.

[42] V. Balasubramanian, B. Craps, J. Hernandez, M. Khramtsov and M. Knysh, *Factorization of the Hilbert space of eternal black holes in general relativity*, 2410.00091.

[43] J.B. Hartle and S.W. Hawking, *Wave Function of the Universe*, *Phys. Rev. D* **28** (1983) 2960.

[44] V. Balasubramanian, A. Lawrence, J.M. Magan and M. Sasieta, *Microscopic Origin of the Entropy of Black Holes in General Relativity*, *Phys. Rev. X* **14** (2024) 011024 [2212.02447].

[45] H. Geng and Y. Jiang, *Microscopic Origin of the Entropy of Single-sided Black Holes*, 2409.12219.

[46] R. Jackiw, *Lower Dimensional Gravity*, *Nucl. Phys. B* **252** (1985) 343.

[47] C. Teitelboim, *Gravitation and Hamiltonian Structure in Two Space-Time Dimensions*, *Phys. Lett. B* **126** (1983) 41.

[48] D. Louis-Martinez, J. Gegenberg and G. Kunstatter, *Exact Dirac quantization of all 2-D dilaton gravity theories*, *Phys. Lett. B* **321** (1994) 193 [gr-qc/9309018].

[49] D. Grumiller, W. Kummer and D.V. Vassilevich, *Dilaton gravity in two-dimensions*, *Phys. Rept.* **369** (2002) 327 [hep-th/0204253].

[50] A. Almheiri and J. Polchinski, *Models of AdS₂ backreaction and holography*, *JHEP* **11** (2015) 014 [1402.6334].

[51] J. Maldacena and D. Stanford, *Remarks on the Sachdev-Ye-Kitaev model*, *Phys. Rev. D* **94** (2016) 106002 [1604.07818].

[52] J. Maldacena, D. Stanford and Z. Yang, *Conformal symmetry and its breaking in two dimensional Nearly Anti-de-Sitter space*, *PTEP* **2016** (2016) 12C104 [1606.01857].

[53] Z. Yang, *The Quantum Gravity Dynamics of Near Extremal Black Holes*, *JHEP* **05** (2019) 205 [1809.08647].

[54] D. Harlow and D. Jafferis, *The Factorization Problem in Jackiw-Teitelboim Gravity*, *JHEP* **02** (2020) 177 [1804.01081].

[55] C.V. Johnson, *Nonperturbative Jackiw-Teitelboim gravity*, *Phys. Rev. D* **101** (2020) 106023 [1912.03637].

[56] D. Stanford and Z. Yang, *Firewalls from wormholes*, 2208.01625.

[57] A. Blommaert, C.-H. Chen and Y. Nomura, *Firewalls at exponentially late times*, 2403.07049.

[58] D. Stanford and L. Susskind, *Complexity and Shock Wave Geometries*, *Phys. Rev. D* **90** (2014) 126007 [1406.2678].

[59] A.R. Brown, D.A. Roberts, L. Susskind, B. Swingle and Y. Zhao, *Holographic Complexity Equals Bulk Action?*, *Phys. Rev. Lett.* **116** (2016) 191301 [1509.07876].

[60] A.R. Brown, D.A. Roberts, L. Susskind, B. Swingle and Y. Zhao, *Complexity, action, and black holes*, *Phys. Rev. D* **93** (2016) 086006 [1512.04993].

[61] P. Caputa, N. Kundu, M. Miyaji, T. Takayanagi and K. Watanabe, *Anti-de Sitter Space from Optimization of Path Integrals in Conformal Field Theories*, *Phys. Rev. Lett.* **119** (2017) 071602 [1703.00456].

[62] P. Caputa, N. Kundu, M. Miyaji, T. Takayanagi and K. Watanabe, *Liouville Action as Path-Integral Complexity: From Continuous Tensor Networks to AdS/CFT*, *JHEP* **11** (2017) 097 [1706.07056].

[63] M. Miyaji, T. Numasawa, N. Shiba, T. Takayanagi and K. Watanabe, *Distance between Quantum States and Gauge-Gravity Duality*, *Phys. Rev. Lett.* **115** (2015) 261602 [1507.07555].

[64] M. Miyaji, *Butterflies from Information Metric*, *JHEP* **09** (2016) 002 [1607.01467].

[65] A. Belin, A. Lewkowycz and G. Sárosi, *Complexity and the bulk volume, a new York time story*, *JHEP* **03** (2019) 044 [1811.03097].

[66] S. Leutheusser and H. Liu, *Causal connectability between quantum systems and the black hole interior in holographic duality*, *Phys. Rev. D* **108** (2023) 086019 [2110.05497].

[67] E. Witten, *Gravity and the crossed product*, *JHEP* **10** (2022) 008 [2112.12828].

[68] V. Chandrasekaran, G. Penington and E. Witten, *Large N algebras and generalized entropy*, *JHEP* **04** (2023) 009 [2209.10454].

[69] G. Penington and E. Witten, *Algebras and States in JT Gravity*, 2301.07257.

[70] E. Witten, *A background-independent algebra in quantum gravity*, *JHEP* **03** (2024) 077 [2308.03663].

[71] J. Kudler-Flam, S. Leutheusser and G. Satishchandran, *Generalized Black Hole Entropy is von Neumann Entropy*, 2309.15897.

[72] J. Kudler-Flam, S. Leutheusser and G. Satishchandran, *Algebraic Observational Cosmology*, 2406.01669.

[73] L. Susskind, *The Typical-State Paradox: Diagnosing Horizons with Complexity*, *Fortsch. Phys.* **64** (2016) 84 [1507.02287].

[74] C. Akers and A. Lucas, *WIP*, .

[75] M. Miyaji, S. Ruan, S. Shibuya and Y. Kazuyoshi, *Non-perturbative Overlaps in JT Gravity*, *To appear* .

[76] M. Miyaji, S. Ruan, S. Shibuya, Y. Kazuyoshi and W. Weng, *WIP*, .

[77] J. Boruch, P. Caputa and T. Takayanagi, *Path-Integral Optimization from Hartle-Hawking Wave Function*, *Phys. Rev. D* **103** (2021) 046017 [2011.08188].

[78] J. Boruch, P. Caputa, D. Ge and T. Takayanagi, *Holographic path-integral optimization*, *JHEP* **07** (2021) 016 [2104.00010].

[79] G. Araujo-Regado, R. Khan and A.C. Wall, *Cauchy slice holography: a new AdS/CFT dictionary*, *JHEP* **03** (2023) 026 [2204.00591].

[80] V. Balasubramanian, P. Caputa, J.M. Magan and Q. Wu, *Quantum chaos and the complexity of spread of states*, *Phys. Rev. D* **106** (2022) 046007 [2202.06957].

[81] V. Balasubramanian, J.M. Magan and Q. Wu, *Quantum chaos, integrability, and late times in the Krylov basis*, 2312.03848.

[82] P. Caputa, H.-S. Jeong, S. Liu, J.F. Pedraza and L.-C. Qu, *Krylov complexity of density matrix operators*, *JHEP* **05** (2024) 337 [2402.09522].

[83] P. Nandy, A.S. Matsoukas-Roubeas, P. Martínez-Azcona, A. Dymarsky and A. del Campo, *Quantum Dynamics in Krylov Space: Methods and Applications*, 2405.09628.